Interferometric Fringe Fluorescence Photobleaching Recovery Interrogates Entire Cell Surfaces

Heidi M. Munnelly,* Deborah A. Roess,§ William F. Wade,# and B. George Barisas*

*Department of Chemistry, Colorado State University, Fort Collins, Colorado 80523; #Department of Microbiology, Dartmouth Medical School, Lebanon, New Hampshire 03756; and §Department of Physiology, Colorado State University, Fort Collins, Colorado 80523

ABSTRACT   Fluorescence photobleaching recovery (FPR) measurements of cell surface protein lateral diffusion typically employ an interrogated spot of 0.5 μm $1/e^2$ radius. The effective spot area represents only 1/500 of the total surface of an 8-μm cell. An FPR measurement of a protein expressed as 50,000 copies per cell reflects the dynamics of 100 molecules. This limits the precision and reproducibility of FPR measurements. We describe a method for interferometric fringe pattern FPR that permits simultaneous interrogation of the entire cell's surface. Fringe patterns are generated interferometrically within the optical path of an FPR system. Methods for interpreting fluorescence recovery kinetics on cells and for determining the protein mobile fraction are presented. With fringe FPR, the murine major histocompatibility complex class II antigen I-A^k expressed on M12.C3.F6 cells has 100-fold improved fluorescence signals relative to spot FPR, with corresponding improvements in signal-to-noise ratios of recovery traces. Diffusion coefficients ($\pm$ standard deviation) of $(2.1 \pm 0.4) \times 10^{-10}$ and $(1.8 \pm 1.0) \times 10^{-10}$ cm^2 s^{-1} with corresponding mobile fractions of I-A^k of $66.1 \pm 7.8\%$ and $63.4 \pm 18.0\%$ were obtained by fringe and spot methods, respectively. The improved reproducibility of fringe over spot results is less than signal improvements predict. There may thus be substantial variation from cell to cell in protein dynamics, and this method may permit the assessment of such variation.

INTRODUCTION

Since the introduction of fluorescence photobleaching recovery by Axelrod et al. (1976) after the pioneering work of Peters and co-workers (Peters et al., 1974) and Jacobson and co-workers (Jacobson et al., 1976), lateral diffusion of cell surface proteins has been commonly measured by spot FPR (see, for example, Qiu et al., 1996). Fully satisfactory results are rarely obtained, however, because of poor signal-to-noise levels, particularly on measurements from poorly expressed cellular proteins. This is due, in large measure, to the fact that a laser beam is focused to a Gaussian spot with a $1/e^2$ radius of 0.5 μm, thus interrogating an area of 0.8 μm^2. If, for example, this spot is used to illuminate the surface of an 8-μm-diameter cell on which $n = 50,000$ copies of the molecule of interest are expressed and fluorescently labeled, calculations show that the number of molecules that provides the FPR signal is $\frac{1}{8}nr_{spot}^2/r_{cell}^2$), or ~100 molecules. If the extent of bleaching is 30%, then one is attempting to measure recovery kinetics from an ensemble of 30 molecules. This tiny sample size accounts in large measure for the very poor signal-to-noise ratios, often as low as 1:1, that can be encountered in FPR studies. As a consequence, large numbers of individual measurements must be averaged. Moreover, the uncertainty in the diffusion coefficient and/or mobile fraction of molecules on any particular cell is so large as to preclude measuring real variation in these parameters from cell to cell.

An enormous improvement in the quality of FPR results, and hence in the applicability of FPR methods, can be afforded by interrogating a substantial fraction of the cell surface at one time. A practical strategy for this involves bleaching a one-dimensional pattern of alternating light and dark areas and interrogating the fluorescence recovery either by uniform illumination or by an attenuated bleaching pattern. Such a fringe pattern can be generated interferometrically. Devaux and co-workers have generated interferometric fringe patterns in a cuvette to measure diffusion of dissolved species (Davoust et al., 1982) and in a microscope to measure diffusion in extended, flat layers of cells or membranes (el Hage Chahine et al., 1993; Morrot et al., 1986). This method has not been applied, however, to single or round cells. McConnell and co-workers (Smith and McConnell, 1978; Smith et al., 1981) have used a Ronchi ruling to achieve pattern photobleaching on microscopic samples, but their method is applicable only to extremely flat samples. In this paper we describe a simple and robust method examining lateral diffusion of species across the entire surface of an individual round cell. The fringe pattern is generated by an interferometer interposed in a laser beam entering a conventional microscope photometer of the type used for spot FPR measurements. This permits easy conversion of the apparatus beween spot and fringe methods.

THEORY

Fringe pattern generation and properties

If two laser beams of wavelength λ intersect at an angle θ, the spacing s of the resulting fringe pattern is given as

$$s = \frac{\lambda/2}{\sin \theta/2} \tag{1}$$

To generate suitable interference patterns on a sample observed in a microscope, all that is necessary is to cause this intersection to occur at some image plane of the sample. If the actual magnification at this plane is related to the objective magnification m by a tube factor t, and if the angle of intersection of the beams is small, then the fringe spacing at the sample is given by

$$s \simeq \frac{\lambda}{mt\theta} \qquad (2)$$

This pattern can be used both to bleach a corresponding region of the sample and to probe the recovery kinetics. The intensity distribution of this pattern is thus described by Eq. 3, where ν, the pattern spacial frequency, is $2\pi/s$:

$$I(x) = I_0 \cos^2 \frac{\nu x}{2};$$

$$= \frac{I_0}{2}(1 + \cos \nu x) \qquad (3)$$

Fluorescence recovery kinetics

If a high-intensity pattern of this type impinges on a fluorescent sample, irreversible photobleaching occurs as a first-order process. The concentration $c(x, 0)$ of labeled material remaining immediately after bleaching over a brief interval is given as

$$c(x, 0) = c_0 \exp\left(-K\frac{1 + \cos \nu x}{2}\right) \qquad (4)$$

where

$$K = \frac{2303\epsilon_M I_0 T\Phi_b \lambda}{Nhc} \qquad (5)$$

Here, ϵ_M is the chromophore molar absorptivity, T is the duration of the bleaching pulse, Φ_b is the quantum yield for bleaching of the chromophore, λ is the wavelength, N is Avogadro's number, h is Planck's constant, and c is the speed of light.

The initial concentration distribution can thus be approximated as

$$c(x, 0) = c_0[a_0(K) + a_1(K)\cos \nu x + a_2(K)\cos 2\nu x + \ldots] \qquad (6)$$

The above constants, $a_0(K)$ and $a_1(K)$, are evaluated by expanding $c(x, 0)$ given in Eq. 4 as a Fourier series and found to involve the modified Bessel functions I_0 and I_1:

$$a_0(K) = \exp\left(-\frac{K}{2}\right)\left(I_0\left(\frac{K}{2}\right)\right) \qquad (7)$$

$$a_1(K) = -2\exp\left(-\frac{K}{2}\right)\left(I_1\left(\frac{K}{2}\right)\right) \qquad (8)$$

The concentration distribution evolves according to a one-dimensional diffusion equation and can be solved by inspection with the result

$$c(x, t) = a_0(K) + a_1(K)\cos \nu x \exp(-\nu^2 Dt) + \ldots \qquad (9)$$

If this distribution is probed with a fringe pattern of the previous form attenuated by a factor f relative to the bleach, we obtain a time-dependent fluorescence signal $F(t)$ given by Eq. 10, where A is the sample area and E is the aggregate excitation and detection efficiency,

$$F(t) = EA\langle c(x, t)fI(x)\rangle$$

$$= \frac{1}{2}EAfI_0c_0a_0(K) + \frac{1}{4}EAfI_0c_0a_1(K)\exp(-\nu^2 Dt) \qquad (10)$$

Fluorescence recovery after photobleaching will thus proceed as a single exponential with a half-time of $0.69/\nu^2 D$, which is completely independent of the extent of bleaching.

Recovery kinetics on spheres

Many of the cells we wish to examine are round lymphoid or other nonadherent cells that assume a spherical shape during examination. The intersection of the fringe pattern with this curved surface produces diffusion of membrane species between bleached regions of differing spacing, giving rise to a distribution of rate constants for fluorescence recovery. This effect can be calculated by considering the cell as a sphere, with the polar axis running perpendicular to the plane of the fringes, i.e., from right to left on the microscope stage. The top and bottom of the cell thus lie along its equator, where the polar angle θ equals $\pi/2$, so that the fringe spacing along this line is simply s and the fluorescence recovery proceeds as $\exp(-\nu^2 Dt) = \exp(-4\pi^2 Dt/s^2)$. More generally, the effective fringe spacing on the cell surface is $s/\sin \theta$, so that recovery occurs as $\exp(-4\pi^2 Dt \sin^2\theta/s^2)$. Thus, where θ is not equal to $\pi/2$, and particularly near the poles of the sphere to the right or left, recovery proceeds more slowly than would be predicted for a flat sample exposed to fringes spaced s apart. The observed recovery signal $F'(t)$ arising from this distribution of exponentials can be evaluated by averaging the fluorescence decay function of Eq. 10, now considered to vary with θ, over the sphere's surface:

$$F'(t) = \frac{1}{2}\int_{\theta=0}^{\theta=\pi} F(t, \theta)\sin \theta \, d\theta$$

$$= \frac{1}{2}EAfI_0c_0a_0(K) + \frac{1}{4}EAfI_0c_0a_1(K) \cdot (\nu^2 Dt)^{-1/2}$$

$$\cdot \left[\frac{1}{2}e^{-\nu^2 Dt}\int_{\theta=0}^{\theta=\pi} e^{\nu^2 Dt\cos^2\theta}\sin \theta \, d\theta\right] \qquad (11)$$

The quantity in brackets is recognized as Dawson's integral of $(v^2 Dt)^{1/2}$ (see table 7.5 in Abramowitz and Stegun, 1968). The normalized recovery kinetics $S(t)$, where $S = 1$ at time 0, can then be numerically evaluated to any desired precision by using this integral. A useful rational approximation for the normalized decay kinetics is found to be

$$S(t) \simeq \frac{1 + 0.385t/t_{1/2}}{1 + 1.032t/t_{1/2} + 0.771(t/t_{1/2})^2} \qquad (12)$$

Thus S decreases toward zero at long times as $1/t$, and the apparent half-time for fluorescence recovery is $1.130 \; s^2/4\pi^2 D$.

Fractional fluorescence recovery

The fractional extent of bleaching B and the fractional fluorescence recovery R after photobleaching are given by

$$B(K) = a_0(0) - a_0(K) - \frac{1}{2}a_1(K) \qquad (13)$$

$$R(K) = -\frac{1}{2}a_1(K)/B(K) \qquad (14)$$

Fluorescence recovery after fringe bleaching proceeds at most one-third of the way back to the prebleach level, and the extent of this recovery depends upon the extent of bleaching, in contrast to spot photobleaching measurements. By eliminating K between Eqs. 13 and 14, one obtains a formula for the fractional fluorescence recovery of a fully mobile species in terms of the extent of bleaching. Equation 15 provides R with a relative error of less than 1.5% for B up to 0.85:

$$R = \frac{1}{3}(1 - 0.15950B + 0.18652B^2 - 0.35594B^3 + \dots) \qquad (15)$$

For comparison, it is valuable to consider the situation for fluorescence recovery when a Gaussian spot of $1/e^2$ radius r_0 is used to bleach and interrogate a fully mobile fluorophore. The kinetics of this recovery takes the particularly simple form of

$$F(t) = F_\infty - (F_\infty - F_0)\frac{t/t_{1/2}}{1 + t/t_{1/2}} \qquad (16)$$

where $t_{1/2}$, the half-time for fluorescence recovery, is $\gamma r_0^2/4D$. The constant $\gamma > 1$ depends upon the extent of bleaching, so that more extensive bleaching leads to proportionately longer recovery times. However, fluorescence recovers fully to the prebleach level, independent of the extent of bleach.

MATERIALS AND METHODS

Chemicals

L-Glutamine, sodium pyruvate, 2-mercaptoethanol, egg phosphatidylcholine, cholesterol, and cardiolipin were purchased from Sigma Chemical Company (St. Louis, MO). Tetramethylrhodamine isothiocyanate (TRITC)

and 1,1'-dioctadecyl-3,3,3',3'-tetramethylindocarbocyanine perchlorate (diI) were purchased from Molecular Probes (Eugene, OR). Fetal bovine serum (FBS) was purchased from Summit Biotechnologies (Fort Collins, CO). RPMI 1640 and penicillin/streptomycin were purchased from Irvine Scientific (Santa Ana, CA). Geneticin (G-418) was purchased from Gibco (Grand Island, NY).

Preparation and fluorescent labeling of liposomes

Liposomes were prepared by a method adapted from that described by Peacock and Barisas (1983). Egg phosphatidylcholine (20 μmol), cholesterol (20 μmol), and cardiolipin (10 μmol) were dissolved in chloroform, placed in a rotary evaporator at 51°C, and purged with nitrogen. The chloroform was allowed to slowly evaporate over the next 60 min. Then 1.5 ml of 2.5% sucrose in phosphate-buffered saline (PBS) was added to the thin lipid layer, and the mixture was allowed to rotate for 5 min at 51°C. Liposomes ranging in size from 1 μm to 5 μm were isolated by centrifugation at $1000 \times g$ for 20 min. Liposomes were labeled with 0.1 mg/ml diI in 95% ethanol for 10 min at 23°C, washed three times with PBS, and suspended in 200 μl of PBS before experiments.

Cell preparation and measurements

M12.C3.F6 cells expressing wild-type I-A^k (Wade et al., 1989a) were grown in RPMI 1640 with 10% FBS, 2 mM L-glutamine, 100 U/ml penicillin, 100 μg/ml streptomycin, 0.1 mM 2-mercaptoethanol, and 300 μg/ml Geneticin (G-418) in 1 mM sodium pyruvate. Typically, 10^6 cells were treated with 0.7 μM (0.13 mg/ml) TRITC-derivatized 39J anti-α^k monoclonal antibody (mAb) for 30 min on ice (Wade et al., 1989b). The 39J anti-α^k mAb was cultured as described by Wade and co-workers (Wade et al., 1989b) and conjugated with TRITC by standard procedures (Brinkley, 1992). Conjugates contained 2.0 mol TRITC per mol 39J antibody. Cells were then washed once with balanced salt solution (BSS) and resuspended in 0.5 ml BSS before the FPR experiment.

FPR instrumentation

Equipment and methods for spot fluorescence photobleaching recovery measurements have been described elsewhere in detail (Young et al., 1994). The apparatus for interference fringe FPR is shown in Fig. 1. The entire optical system is mounted on a 5 ft $\times$ 10 ft Newport Research Corporation laser table. A Coherent Radiation Innova 100 argon ion laser provides excitation at 488 nm for fluorescein-conjugated proteins and at 514 nm for tetramethylrhodamine-conjugated proteins. The beam passes into a light pulse generator, where it is separated into two components, one of which is attenuated 300- to 3000-fold by two reflections off unsilvered surfaces. The unattenuated beam is normally blocked by an electronic shutter. The beams are recombined by a beam splitter, and bleaching pulses of 5 ms to 8 s are produced by opening the electronic shutter. The bleaching and interrogation beam intensities are independently adjustable, and no optical components move during the operation of the device. Beam alignment of ± 2 arc sec is achieved in practice (Barisas, 1980). A small Michelson interferometer is inserted between the pulse generator and the microscope. This device employs five first-surface mirrors and one polarization-preserving beam splitter cube to divide the collimated laser beam into two equal intensity components separated by a center-to-center distance variable from 1 to 10 mm and adjustable for convergence at any point beyond the interferometer. There is essentially no optical path difference between the two beams. For spot FPR measurements this interferometer is removed, and a 150-mm lens is used to focus the laser beam at a spot coincident with an image plane of the microscope located behind the entrance port for the fluorescence vertical illuminator. The tube factor at this plane is 1.106. For fringe measurements the interferometer is placed in the laser beam path, and beams are adjusted for superimposition at this image plane. Fringe spacing is controlled by measuring and adjusting the

FIGURE 1 Apparatus for fluorescence photobleaching recovery measurement of cell surface protein lateral diffusion, using interferometrically generated fringes. The functions of the various components are described in the text. Note the convenient placement of the interferometer for easy conversion from the spot mode to the fringe mode.
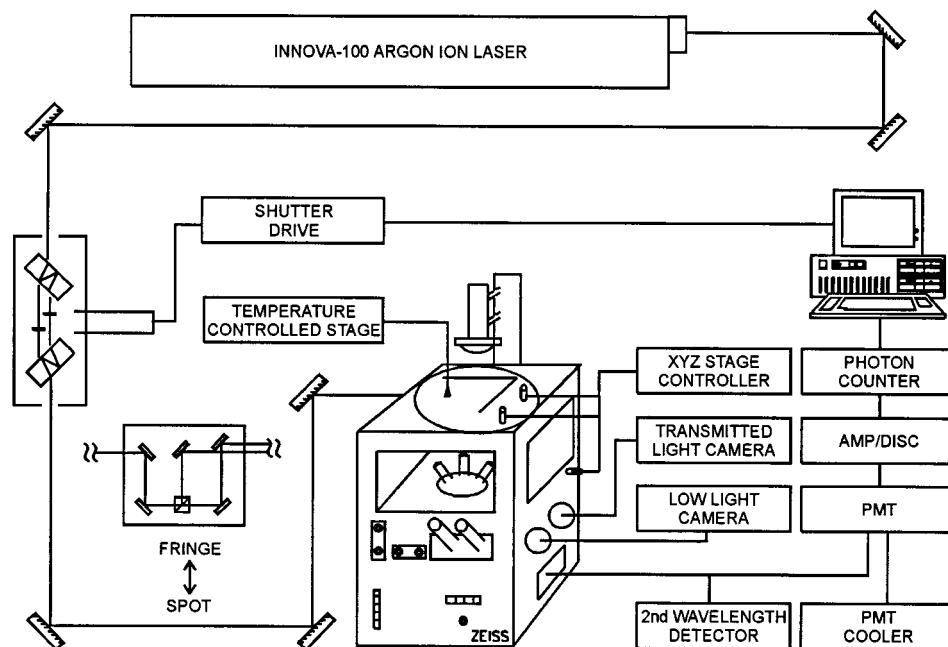
angle of beam intersection, and small adjustments in fringe orientation can be accomplished. By proper selection of the laser beam diameter, the focusing lens focal length (spot mode), and the beam intersection angle (fringe mode), one can achieve equal recovery times for fluorescent species on spherical samples. If the recovery half-times for the spherical fringe mode ($1.130\ s^2/4\pi^2 D$; Eq. 12) and the spot mode ($r^2/4D$; Eq. 16) are equated, it is seen that equal recovery times are observed when

$$S = 1.06R\left(\frac{d}{f}\right) \qquad (17)$$

where S is the spacing between interferometer beams at a distance d (~ 1 m) from their intersection, f is the focal length of the focusing lens for spot measurements, and R is the $1/e^2$ laser beam radius. This is exceptionally convenient for comparative measurements and is the way our system is normally configured, i.e., with the beam spacing at the interferometer approximately equal to seven times the laser beam $1/e^2$ radius.

The microscope photometer is based on the Zeiss Axiomat microscope equipped with a fluorescence vertical illuminator and with an MP03 photometer module. Light entry into the vertical illuminator is controlled by a polarization-preserving beam splitter that permits selection of either the laser beam for fluorescence photobleaching recovery measurements or light from a 100-W Hg arc for general immunofluorescence. Our normal objective in these studies is a Zeiss 63× Plan Neofluar immersion fluorescence objective of NA 1.00. Standard Zeiss barrier and exciter filters are used, but Omega dichroic mirrors 510DRLPO2 and 540DRLPO2 are essential for fluorescein and tetramethylrhodamine measurements, respectively. Many other filters produced irregular interference patterns of low modulation depth when only one of the interferometer's two beams was allowed into the microscope. Cells are examined under a coverslip on well slides, and the temperature is maintained by a thermoelectrically cooled/heated thermal stage with a temperature range of 0°C to 40°C. An MP03 photometer provides the ability to observe visually the greater part of the microscopic field while directing fluorescence emitted from the rectangular regions of independently varying x and y dimensions to the photomultiplier. The objective rear focal plane is imaged on the photocathode of a selected Hamamatsu R943 photomultiplier. An electronic shutter ahead of the photomultiplier protects it from damaging levels of illumination during both bleaching and sample examination by transmitted light. A thermoelectrically cooled housing (Products for Research, Danvers, MA) maintains the photocathode at −30°C, affording dark count rates of 10 cps.

Photomultiplier output is fed to a PAR 1180 preamplifier and then to a custom photon counting card contained in a PC Pentium computer. Digital output from the card controls the electronic shutters. Thus all experimental and data-taking functions are under program control. An image intensification system facilitates accurate focusing of the laser beam on the faintly fluorescent cell surfaces.

Conditions for photobleaching measurements

For spot measurements on cells with a 63× objective, an image plane aperture of 0.13×0.13 mm was used, which conveniently accommodates the 0.47 μm $1/e^2$ spot radius illuminated by the focused laser beam. For the cell experiments, power in the bleaching pulse was 4 mW and, in the probe beam, 9 μW. For the fringe measurements on cells, the region illuminated at the sample had a $1/e^2$ radius of 19 μm and a photometer acceptance region large enough to encompass the entire cell. Because of the larger interrogated area, much higher total powers were needed, namely 1.3 W in the bleaching pulse and 3 mW in the probe beam. The fringe spacing was ~1.6 μm. Fringe and spot FPR bleaching times were 350 ms and 100 ms, respectively, with typical experiment run times of 15 s prebleach and 25 s postbleach, with 50 ms/pt data acquisition. Measurements were performed at 23°C for all samples. Slightly different conditions were used for liposome measurements (see Table 1).

Data analysis

FPR data are processed on-line. Actual processing takes place in Turbo Pascal, with machine language subroutines providing communication with the photon counting card. A photobleaching run on an individual cell is initiated by a call from the main program, which activates the photon counter. After at least 16 points have been obtained to establish the prebleach fluorescence, a call to the shutter synchronizer requests a bleaching pulse. When the pulse sequence is complete, data points are recorded to delineate fluorescence recovery kinetics. Equations 16, 10, and 11, respectively, define fluorescence recovery kinetics for spot photobleaching and for fringe photobleaching of planar and spherical samples. Our procedure is to represent the unadjusted raw data directly in terms of the various parameters associated with a given measurement. These parameters include the prebleach and immediate postbleach fluorescence levels F_o and

F_- (which together determine K), the extent of mobile fluorophores M on the time scale of the experiment, and an appropriate function (spot, flat fringe, spherical fringe, etc.) representing the recovery kinetics in terms of a decay half-time $t_{1/2}$. We evaluate the parameters directly by the Marquardt nonlinear least-squares algorithm (Bevington, 1969). K, in turn, is used to calculate γ for spot measurements or the predicted mobility M for fringe measurements. From the measured time $t_{1/2}$ at which fluorescence recovery is half-complete, and from the known optical parameters, the desired diffusion constant can then be evaluated. This method of analysis is extremely fast in computer execution, fits all of the available data directly as observed, and allows a single operating program to analyze FPR data obtained in a variety of experimental configurations. Because the observed fluorescence values are obtained by photon counting, Poisson statistics apply, and each point is assigned a statistical weight inversely proportional to its own magnitude. For data in perfect agreement with the models, a reduced χ^2 value equal to the number of points taken minus four is expected. We accept only bleaches where reduced χ^2 is no more than twice this ideal value and typically examine 10–20 cells per point.

RESULTS AND DISCUSSION

Spot and fringe FPR recovery kinetics

Fig. 2 shows calculated normalized recovery kinetics for photobleaching with a Gaussian spot and with fringe patterns on flat and spherical samples. All traces have the same half-time. At short times, both fringe traces recover comparably as $\exp(-\nu^2 Dt)$, and these kinetics are faster than those exhibited by the spot. At long times, fringes on a spherical sample exhibit the slowest recovery, which arises from widely spaced fringes at the right and left ends of the cell.
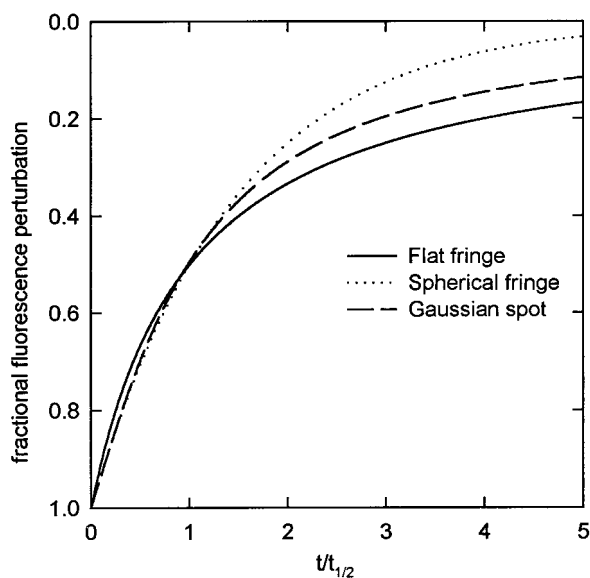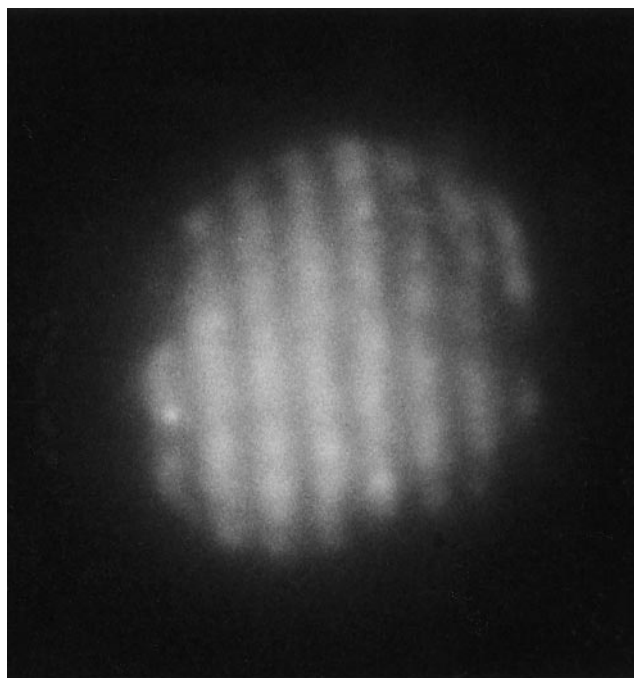

FIGURE 3   Fluorescence photomicrograph of a three-dimensional interference pattern on an M12.C3.F6 cell labeled with TRITC-succinyl concanavalin A. The interferometer was set to yield a fringe spacing of 1.75 μm. The cell's diameter is $\sim$12 μm, so seven or eight fringes illuminate the cell surface.

Generation of interference pattern on cell surfaces

Fig. 3 shows the interferometrically generated fringe pattern illuminating an M12.C3.F6 lymphoma cell heavily labeled with TRITC-succinyl concanavalin A to provide a clear visualization of the fringes. Patching of membrane glycoproteins by the lectin causes the observed irregularity in surface fluorescence. The cell is $\sim$12 μm in diameter, and about seven fringes are clearly visible on the cell's surface. The three-dimensional structure of the fringe pattern on the microscope stage is illustrated in Fig. 4. The x axis denotes displacement on the sample right or left of the microscope

FIGURE 2   Theoretical fluorescence recovery curves for Gaussian spot, flat fringe, and spherical fringe optical geometries. The y axis shows the fluorescence perturbation normalized between 1.0 and 0, and the x axis shows the evolution of the recovery traces over time with respect to the recovery half-time $t_{1/2}$. All three traces have the same $t_{1/2}$, but each behaves differently at long and short times.
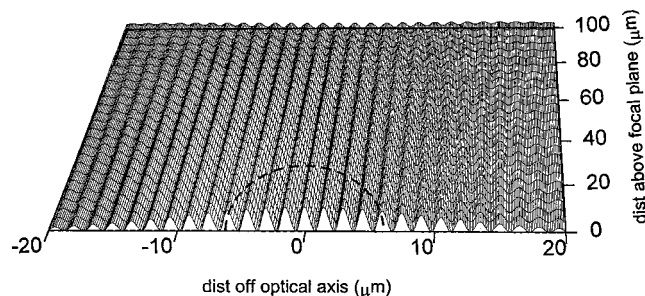

FIGURE 4   Light intensity distribution in a three-dimensional interference pattern at the microscope stage. The interference pattern was calculated with a fringe spacing of 1.6 μm and a $1/e^2$ radius of 18 μm. A cell 12 μm in diameter centered within the interference pattern would be evenly illuminated by the striped pattern.

TABLE 1 Diffusion parameters measured by fringe and spot FPR methods on dil-labeled liposomes*

	Fringe FPR[#]	Spot FPR[§]
D (10^{-9} cm^2 s^{-1})	3.5 ± 0.8[¶]	4.1 ± 0.8[¶]
Mobility (%)	93.8 ± 3.7	92.7 ± 2.2

*Liposomes prepared from egg phosphatidylcholine, cholesterol, and cardiolipin with a ratio of 2:2:1.

[#]Fringe mode instrument conditions: probe power 250 μW, bleach power 650 mW, bleach duration 75 ms, channel width 10 ms/channel, experiment run times 5 s prebleach and 10 s postbleach, fringe spacing 1.3 μm, 63× objective, temperature 23°C.

[§]Spot mode instrument conditions: probe power 6 μW, bleach power 16 mW, bleach duration 10 ms, channel width 10 ms/channel, experiment run times 5 s prebleach and 10 s postbleach, 0.48 μm $1/e^2$ spot diameter, 63× objective, temperature 23°C.

[¶]Mean and standard error of the mean for a set of seven measurements.

optical axis, and the y axis indicates displacement above the level of beam crossing in the sample. The mesh height indicates fringe pattern intensity. The data are calculated for a fringe spacing at the sample of 1.6 μm and a $1/e^2$ beam radius of 18 μm. A cell can thus be evenly illuminated with a three-dimensional fringe pattern that passes through the cell like an egg slicer. Because the pattern has a depth of field substantially greater than the cell thickness, light intensity at any point on or in the sample is essentially constant.

Fringe versus spot FPR methods

Fringe FPR measurements of diI diffusion on liposomes agree well with spot FPR measurements. This provides the most convincing validation that the fringe and spot measurements yield comparable diffusion parameters. Table 1 shows the diffusion parameters for diI, where the average diffusion coefficients (± standard error of the mean) of $(3.5 \pm 0.8) \times 10^{-9}$ and $(4.1 \pm 0.8) \times 10^{-9}$ cm^2 s^{-1} and percentage mobile fractions (± standard error of the mean) of 93.8 ± 3.7% and 92.7 ± 2.2% were measured by fringe and spot methods, respectively. The levels of precision of

these measurements are comparable, because diI-labeled liposomes provide enough fluorescence signal to saturate the detector in both the spot and the fringe measurements. These results are comparable to diI diffusion results obtained in previous liposome studies (Fahey and Webb, 1978; Peacock and Barisas, 1983).

On cells the fringe method yields a vast improvement in fluorescence recovery signals. Fig. 5 illustrates a comparison of fringe and spot FPR data obtained on individual cells in the same instrument at equal probe beam intensities. Wild-type MHC class II antigen I-A^k on M12.C3.F6 cells was labeled with TRITC-39J anti-α^k mAb. It is apparent from Fig. 5 and Table 2 that fringe measurements afford 100-fold enhanced signal relative to the spot method, with corresponding improvement in recovery trace signal-to-noise ratios.

Fringe measurements of diffusion coefficients on cells also agree well with spot FPR measurements. Numbers obtained from analysis of the one fringe recovery trace and the one spot recovery trace on M12.C3.F6 cells in Fig. 5 are shown in Table 2. The averaged fringe and spot measurements made in these experiments yield diffusion coefficients (± standard error of the mean) of $(2.07 \pm 0.11) \times 10^{-10}$ and $(1.99 \pm 0.23) \times 10^{-10}$ cm^2 s^{-1}, respectively, and the two measurements agree to within experimental error. These values also agree with those of Wade and co-workers, who measured a lateral diffusion coefficient of 2×10^{-10} cm^2 s^{-1} for the wild-type MHC class II antigen with the spot FPR method (Wade et al., 1989b).

Fringe FPR measurements may yield diffusion parameters reproducible enough to identify cell-to-cell variation. The data in Table 3 compare the reproducibility of fringe and spot measurements of wild-type I-A^k lateral diffusion on M12.C3.F6 cells. Cells were labeled with TRITC-39J anti-α^k mAb, and 12 cells were examined by each method. The measured diffusion constant and mobile fraction of the labeled protein are tabulated for each cell examined; the errors cited are the statistical uncertainties of the fit for each parameter. The statistics of each group of measurements are
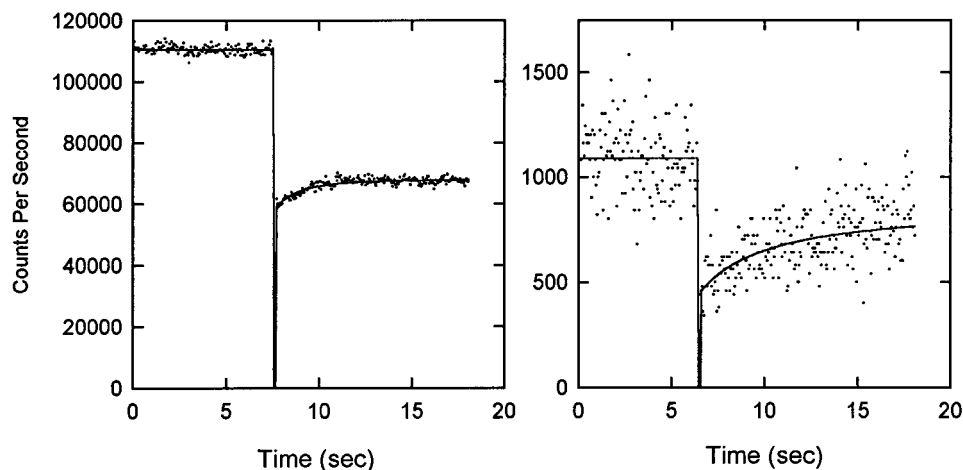

FIGURE 5 Comparison of fringe (*left*) and spot (*right*) photobleaching recovery traces on comparable M12.C3.F6 cells labeled with TRITC-39J anti-α^k mAb. The fringe method yields a ~100-fold improvement in fluorescence signals, as well as a corresponding improvement in the trace signal-to-noise ratio.

TABLE 2 Diffusion parameters evaluated for wild-type I-A^k on M12.C3.F6 cells from a single fringe and a single spot recovery trace (from Fig. 5)*

	Fringe FPR[#]	Spot FPR[§]
D (10^{-10} cm^2 s^{-1})	2.3 ± 0.3[¶]	1.9 ± 0.8[¶]
Mobility (%)	60.3 ± 1.2	65.1 ± 2.5
Bleach (%)	46.7	58.8
Initial fluor (cps)	110,706	1,041

*Cells labeled with 0.7 μM TRITC-39J mAb.

[#]Fringe mode instrument conditions: probe power 3 mW, bleach power 1.3 W, bleach duration 350 ms, channel width 50 ms/channel, fringe spacing 1.3 μm, 63× objective, temperature 23°C.

[§]Spot mode instrument conditions: probe power 4 μW, bleach power 10 mW, bleach duration 100 ms, channel width 50 ms/channel, 0.48 μm $1/e^2$ spot diameter, 63× objective, temperature 23°C.

[¶]Errors cited as the statistical uncertainties of the fit for each parameter.

also tabulated. It is clear that the reproducibility of diffusion parameters obtained by fringe methods is vastly better than those obtained by spot techniques. For example, the standard deviation of fringe diffusion coefficients is 0.37×10^{-10} cm^2 s^{-1}, almost three times lower than the 0.97×10^{-10} cm^2 s^{-1} obtained by spot methods. This improvement is, however, not as large as the 100-fold improved signal levels would suggest. Fringe measurements may thus be useful in identifying real cell-to-cell variation in protein diffusional parameters.

Fringe measurements require attention to specific technical issues. High laser powers (>2 W) are required, so laser stability is a more serious concern than in spot measurements. With the use of much higher laser powers required in the fringe mode, photomultiplier saturation can become an issue, particularly when lipid diffusion measurements are performed. Furthermore, fluorescence recovers at most 33%

of the way back to the prebleach level, complicating the measurement of protein fractional mobility. Finally, signal contribution from cytoplasmic autofluorescence may be substantial, but subtraction of recovery curves obtained on unlabeled cells from labeled cell recovery curves reduces the effect of autofluorescence on the recovery kinetics to zero.

In conclusion, we have shown that interferometric fringe FPR provides significant advantages over conventional spot FPR methods. First, lateral diffusion information is obtained from molecules across the entire three-dimensional surface of the cell. Thus signals are typically 100-fold higher than spot methods, with corresponding improvements in signal-to-noise ratios of recovery traces. The method therefore allows membrane dynamics of weakly expressed proteins on transfected cells to be measured where, with spot methods, useful results could not be obtained. Moreover, the measured recovery kinetics are independent of the extent of bleaching, which contributes to increased precision in the measurement of diffusion coefficients. For these various reasons, precision of diffusion parameters obtained from individual cells may be high enough to allow identification of cell-to-cell variation in protein mobility.

TABLE 3 Comparison of fringe and spot FPR measurements of wild-type I-A^k lateral diffusion on individual M12C3.F6 cells*

	Fringe FPR[#]		Spot FPR[#]	
	D (10^{-10} cm^2 s^{-1})	M (%)	D (10^{-10} cm^2 s^{-1})	M (%)
	1.77 ± 0.47[§]	61.3 ± 6.8[§]	1.31 ± 0.72[§]	41.6 ± 5.8[§]
	2.28 ± 0.29	71.5 ± 12.0	1.54 ± 0.26	86.4 ± 6.0
	2.27 ± 0.22	59.1 ± 7.5	1.29 ± 0.48	65.8 ± 7.0
	2.43 ± 0.32	67.8 ± 27.6	1.07 ± 0.23	44.1 ± 2.6
	2.18 ± 0.49	65.7 ± 18.8	2.00 ± 0.66	75.9 ± 23.2
	1.77 ± 0.41	72.0 ± 21.1	1.86 ± 0.81	65.1 ± 24.9
	2.00 ± 0.45	68.0 ± 20.3	1.28 ± 0.30	49.3 ± 4.9
	2.55 ± 0.24	62.4 ± 7.8	4.10 ± 0.87	46.7 ± 2.3
	1.88 ± 0.25	59.8 ± 3.5	3.37 ± 2.17	50.0 ± 13.3
	1.71 ± 0.22	61.9 ± 3.4	1.61 ± 0.36	79.7 ± 5.7
	1.42 ± 0.25	85.9 ± 40.2	1.07 ± 0.27	59.6 ± 7.1
	2.60 ± 0.35	57.9 ± 10.7	1.02 ± 0.17	96.1 ± 8.9
Mean[¶]	2.07	66.1	1.79	63.4
σ[¶]	0.37	7.8	0.97	18.0

*Cells labeled with 0.7 μM TRITC-39J mAb.

[#]Instrument settings and laser powers for the fringe and spot modes are described in the text.

[§]Errors cited as the statistical uncertainties of the fit for each parameter.

[¶]Mean and standard deviation of the measured diffusion parameters.

REFERENCES

Abramowitz, M., and I. A. Stegun. 1968. Handbook of Mathematical Functions. Dover Publications, New York.

Axelrod, D., D. E. Koppel, J. Schlessinger, E. Elson, and W. W. Webb. 1976. Mobility measurement by analysis of fluorescence photobleaching recovery kinetics. *Biophys. J.* 16:1055–1069.

Barisas, B. G. 1980. Criticality of beam alignment in fluorescence photobleaching recovery experiments. *Biophys. J.* 29:545–548.

Bevington, P. R. 1969. Data Reduction and Error Analysis for the Physical Sciences. McGraw-Hill Book Company, New York.

Brinkley, M. A. 1992. A brief survey of methods for preparing protein conjugates with dyes, haptens, and cross-linking reagents. *Bioconjug. Chem.* 3:2–13.

Davoust, J., P. F. Devaux, and L. Leger. 1982. Fringe pattern photobleaching, a new method for the measurement of transport coefficient of biological macromolecules. *EMBO J.* 1:1233–1238.

el Hage Chahine, J. M., S. Cribier, and P. F. Devaux. 1993. Phospholipid transmembrane domains and lateral diffusion in fibroblasts. *Proc. Natl. Acad. Sci. USA.* 90:447–451.

Fahey, P. F., and W. W. Webb. 1978. Lateral diffusion in phospholipid bilayer membranes and multilamellar liquid crystals. *Biochemistry.* 17:3046–3053.

Jacobson, K., Z. Derzko, E.-S. Wu, Y. Hou, and G. Poste. 1976. Measurement of the lateral mobility of cell surface components in single, living cells by fluorescence recovery after photobleaching. *J. Supramol. Struct. Cell. Biochem.* 5:565–576.

Morrot, G., S. Cribier, P. F. Devaux, D. Geldwerth, J. F. Bureau, P. Fellmann, P. Herve, and B. Frilley. 1986. Asymmetric lateral mobility of phospholipids in human erythrocyte membrane. *Proc. Natl. Acad. Sci. USA.* 83:6863–6867.

Peacock, J. S., and B. G. Barisas. 1983. Photobleaching recovery studies of T-independent antigen mobility on antibody-bearing liposomes. *J. Immunol.* 131:2924–2929.

Peters, R., J. Peters, K. H. Tews, and W. Bahr. 1974. A microfluorimetric study of translational diffusion in erythrocyte membranes. *Biochim. Biophys. Acta.* 367:282–294.

Qiu, Y., W. F. Wade, D. A. Roess, and B. G. Barisas. 1996. Lateral dynamics of major histocompatibility complex class II molecules bound with agonist peptide or altered peptide ligands. *Immunol. Lett.* 53:19–23.

Smith, B. A., and H. M. McConnell. 1978. Determination of molecular motion in membranes using periodic pattern photobleaching. *Proc. Natl. Acad. Sci. USA.* 75:2759–2763.

Smith, L. M., H. M. McConnell, B. A. Smith, and J. W. Parce. 1981. Pattern photobleaching of fluorescent lipid vesicles using polarized laser light. *Biophys. J.* 33:139–146.

Wade, W. F., Z. Z. Chen, R. Maki, S. McKercher, E. Palmer, J. C. Cambier, and J. H. Freed. 1989a. Altered A-I protein-mediated transmembrane signaling in B cells that express truncated I-A^k protein. *Proc. Natl. Acad. Sci. USA.* 86:6297–6301.

Wade, W. F., J. H. Freed, and M. Edidin. 1989b. Translational diffusion of class II major histocompatibility complex molecules is constrained by their cytoplasmic domains. *J. Cell Biol.* 109:3325–3331.

Young, R. M., J. K. Arnette, D. A. Roess, and B. G. Barisas. 1994. Quantitation of fluorescence energy transfer between cell surface proteins via fluorescence donor photobleaching kinetics. *Biophys. J.* 67: 881–888.